Oncogene (2005) 24, 2512–2524

www.nature.com/onc

EWS-FLI1 target genes recovered from Ewing's sarcoma chromatin

Christine Siligan[1], Jozef Ban[1], Radostina Bachmaier[1], Laura Spahn[1], Michael Kreppel[1], Karl-Ludwig Schaefer[2], Christopher Poremba[2], Dave NT Aryee[1] and Heinrich Kovar*[,1]

[1]*Children's Cancer Research Institute (CCRI), St Anna Kinderspital, Kinderspitalgasse 6, Vienna A1090, Austria;* [2]*Institute of Pathology, Heinrich-Heine-University, Moorenstrasse 5, Dusseldorf 40225, Germany*

In all, 85% of Ewing's sarcoma family tumors (ESFT), a neoplasm of unknown histogenesis, express *EWS-FLI1* transcription factor gene fusions. To characterize direct target genes avoiding artificial model systems, we cloned genomic DNA from ESFT chromatin precipitating with EWS-FLI1. We now present a comprehensive list of 99 putative transcription factor targets identified, for the first time, by a hypothesis-free approach based on physical interaction. Gene-derived chromatin fragments co-precipitating with EWS-FLI1 were nonrandomly distributed over the human genome and localized predominantly to the upstream region and the first two introns of the genes. At least 20% of putative direct EWS-FLI1 targets were neural genes. One-third of genes recovered showed a significant ESFT-specific expression pattern and were found to be altered upon RNAi-mediated knockdown of EWS-FLI1. Among them, *MK-STYX*, encoding a MAP kinase phosphatase-like protein, was consistently expressed in ESFT. EWS-FLI1 was found to drive *MK-STYX* expression by binding to a single ETS binding motif within the first gene intron. *MK-STYX* serves as precedence for successful recovery of direct EWS-FLI1 targets from the authentic ESFT cellular context, the most relevant system to study oncogenic mechanisms for the discovery of new therapeutic targets in this disease.
Oncogene (2005) **24,** 2512–2524. doi:10.1038/sj.onc.1208455
Published online 14 February 2005

Keywords: chromatin immunoprecipitation; Ewing's sarcoma; EWS-FLI1; MAP kinase phosphatase; RNA interference

Introduction

Ewing's sarcoma family tumors (ESFT) are characterized in about 85% of cases by a reciprocal chromosomal translocation fusing the human *ETS* oncogene *FLI1* to the *EWS* gene (Delattre *et al*., 1994). As a result, a chimeric protein is expressed, which is commonly assumed to act as an aberrant transcription factor (Ohno and Reddy, 1993; Bailly *et al*., 1994; Lessnick *et al*., 1995). So far, the study of EWS-FLI1 downstream pathways has been largely restricted to heterologous cell types ectopically expressing the fusion protein since the tissue of origin for ESFT is still unknown. Gene expression profiling in different model systems revealed an almost equal number of genes suppressed as activated in response to ectopic EWS-FLI1 expression (Arvand *et al*., 2001; Dauphinot *et al*., 2001; Lessnick *et al*., 2002; Rorie *et al*., 2004). Several potential candidates have been described as being specifically affected by EWS-FLI1. These include genes encoding cytoskeletal and extracellular matrix proteins as well as proteins involved in their degradation (Braun *et al*., 1995; Fuchs *et al*., 2003; Matsui *et al*., 2003), several genes involved in intra- or extracellular signaling (Thompson *et al*., 1996; May *et al*., 1997; Hahm *et al*., 1999; Im *et al*., 2000; Deneen *et al*., 2003a; Watanabe *et al*., 2003; Fuchs *et al*., 2004), and cell cycle regulation and senescence (Watson *et al*., 1997; Arvand *et al*., 1998; Dauphinot *et al*., 2001; Lessnick *et al*., 2002; Deneen *et al*., 2003a; Nakatani *et al*., 2003; Takahashi *et al*., 2003). For few genes (*MNFG*, *PIM-3*) forced expression has been shown to support transformation of NIH3T3 cells (May *et al*., 1997; Deneen *et al*., 2003b). The differential screening methods applied in these studies did not allow discrimination between direct and indirect targets of EWS-ETS chimeric proteins. In addition, depending on the model system, EWS-FLI1 expression resulted in diverse cell-type-specific physiological outcomes ranging from cell death or growth arrest (Deneen and Denny, 2001; Lessnick *et al*., 2002) to blocked or altered differentiation (Teitell *et al*., 1999; Eliazer *et al*., 2003; Torchia *et al*., 2003; Rorie *et al*., 2004) or transformation (May *et al*., 1993b; Lessnick *et al*., 1995), while certain non-NIH3T3 fibroblast cell lines appeared not to be affected by EWS-FLI1 expression at all (May *et al*., 1993a). These functional discrepancies are reflected by differences in putative EWS-FLI1 target gene expression patterns as demonstrated recently for *PDGF-c* (Zwerner *et al*., 2003). As a consequence, only few candidate genes (*TGFβR2*, *ID-2*, *TNC*, *UPP-1*) have been confirmed as directly regulated by EWS-ETS fusion proteins in ESFT so far (Hahm *et al*., 1999; Im *et al*., 2000; Nishimori *et al*., 2002; Deneen *et al*., 2003a; Fukuma *et al*., 2003; Watanabe *et al*., 2003).

In order to identify direct EWS-FLI1 target genes by a hypothesis-free approach, which is independent of the

*Correspondence: H Kovar;E-mail: heinrich.kovar@ccri.univie.ac.at
Received 8 September 2004; revised 10 December 2004; accepted 10 December 2004; published online 14 February 2005

mode of gene regulation, we chose chromatin immunoprecipitation (ChIP) (Weinmann and Farnham, 2002) to enrich for and clone genomic DNA associated with EWS-FLI1 in the authentic ESFT cellular context.

Results

A dual ChIP approach enriches for EWS-FLI1-specific target sequences

To precipitate EWS-FLI1-containing chromatin complexes, specific antibodies against the C-terminal FLI1 and the N-terminal EWS portions were used in two successive rounds of ChIP. Control precipitations were performed in the absence of an antibody and in the presence of an irrelevant antibody of the same isotype (anti-KAI1). ChIP experiments were performed in the ESFT cell line STA-ET-7.2, which lacks germline EWS and FLI1 expression (Kovar *et al*., 2001).

Genomic DNA was directly cloned from EWS-FLI1-containing chromatin complexes. Control precipitates were equally treated. About 400 insert-containing clones were obtained for the specific antibodies as opposed to 100 and 50 clones for the unrelated antibody sample and the no-antibody control, respectively. Inserts larger than 150 bp were sequenced; 278, 49, and 10 clones obtained from ChIP with EWS-FLI1 specific, irrelevant and no antibody were analysed in detail.

Nonspecific precipitation of DNA fragments would be expected to result in about 20% of gene hits, as this is the percentage of genomic DNA covered by genes according to the draft human genome sequence. Reminiscent of a random precipitation, the frequency of gene-derived clones obtained from ChIP with the irrelevant antibody was 18% (9/49), and in the sample precipitated in the absence of any antibody, only 1 of 10 cloned fragments was derived from a gene. In contrast, EWS-FLI1-specific antibodies specifically enriched in gene hits (including 10 kb of upstream and downstream sequences) with a frequency of 39% (108/278). Nine genes were hit twice. Since no amplification reaction has been performed before cloning, these clones represent independent hits. Thus, we identified a total of 99 genes as potential EWS-FLI1 binders (Table 1).

Genomic assignments of EWS-FLI1-specific ChIP clones

The chromosomal localizations of the 170 EWS-FLI1-associated intergenic clones largely followed the proportional genomic share of the individual chromosomes considering their size and number in the published karyotype of the STA-ET-7.2 cell line (Hattinger *et al*., 1999). This suggests a random distribution that is compatible with nonspecific precipitation (data not shown). In contrast, the chromosomal distribution of the 99 genes co-precipitating with the EWS-FLI1-specific antibodies did not reflect the chromosomal gene content, with an over-representation of genes encoded on chromosomes 3 and 8. Otherwise, genes hit by EWS-FLI1-specific ChIP were found on all chromosomes except 14, 21, and 22 (data not shown).

Figure 1 illustrates the intragenic distribution of gene-derived fragments cloned from the EWS-FLI1-specific ChIP samples. In all, 12 of the 99 cloned gene fragments localized to the upstream region (up to 10 kb from exon 1); 27 and 18 fragments were derived from introns/exons 1 and 2, respectively. Thus, 58% of EWS-FLI1-specific intragenic ChIP clones localized to gene regions likely involved in transcriptional regulation.

Regulation of EWS-FLI1-specific genes by RNAi-mediated suppression of EWS-FLI1

The impact of EWS-FLI1 binding on expression of its putative direct target genes was studied in STA-ET-7.2 cells after modulation of EWS-FLI1 by RNA interference (RNAi). Two specific small interfering (si) RNAs, one targeting the fli1 3′ coding region (EF4) and one targeting the fusion region of type 2 ews-fli1 RNA (EF22), the variant expressed in STA-ET-7.2 cells, as well as a type 1 fusion-specific siRNA (EF30) were designed and cloned as small hairpin (sh) precursor RNA encoding cassettes into the retroviral vector pSR. As demonstrated in Figure 2, shRNAs targeting type 2 EWS-FLI1 efficiently interfered with growth of STA-ET-7.2 cells. In monolayer cultures (Figure 2a), doubling times for shRNA-silenced cells were more than 4 days, while control-infected cells doubled within about 24 h. Colony formation of EWS-FLI1-silenced cells in soft agar was completely suppressed. Even after 11 days postinfection (8 days after plating), no multicellular colonies were observable, while control-infected cells efficiently formed colonies comprising more than four cells at a frequency of 2.7%. However, 2 days later, when the number of control-infected colonies was 5.8 per 100 seeded cells, small colonies were also observed in shEF4- and shEF22-infected cells at a frequency of 0.1%, indicating that EWS-FLI1 silencing did not eradicate the cells (not shown). Figures 2c and d demonstrate efficient suppression of *EWS-FLI1* expression by the construct shEF4 6 days after retroviral infection of STA-ET-7.2 cells and its effect on the regulation of known EWS-FLI1 downstream genes. Concomitant with *EWS-FLI1* modulation, expression of *TGFβR2* and $p57^{KIP2}$, two genes known to be suppressed in the presence of EWS-FLI1, increased dramatically, and *CCND1* expression decreased. Similar results were obtained with the construct shEF22 (data not shown).

Affymetrix GeneChip analysis was conducted in STA-ET-7.2 cells using the HG-U133A and B microarrays to study the influence of EWS-FLI1 suppression on the expression of the putative EWS-FLI1 target genes obtained by ChIP. Three independent comparisons were performed between EWS-FLI1-suppressed (shEF4 and shEF22) and mismatch (shEF30) or empty control vector (pSR)-containing cells. To validate the functional effect of EWS-FLI1 suppression, we investigated changes in expression of the established target genes *TGFβR2* and *TNC* (Figure 3a). As expected, tnc mRNA

Table 1 EWS-FLI1-specific genes identified by ChIP in STA-ET-7.2 cells

Gene	*Localization*		*RNAi*		*ESFT/non-ESFT*	*Function*
	Chromosome	*Gene*	*Fold decrease*		*Median ratio*	
			M	*s.d.*		
(a) Downregulation upon repression by EWS-FLI1-specific shRNA						
ACCN1	17q11.2	int1	4.61	1.82	0.67	Neuronal sodium channel1
ASNS	7q21.3	2.5 kb up	1.96	0.44	0.79	Asparagine synthetase
CDC14B	9q22.32	int1	1.56	0.08	0.54	CDC14 cell division cycle 14 homolog
CLASP2	3p22.3	int10	1.67	0.19	1.44	CLIP-associating protein family member
CNTNAP2	7q35	int17	2.28	0.80	2.08	Contactin-associated protein like
DLG2	11q14.1	int2	3.24	1.06	7.94	Discs, large homolog 2
GTF2E2#	8p21	3 kb up	1.26	0.14	1.98	General transcription factor IIE
IDH3B	20p13	10 kb dw	1.41	0.15	1.66+	Isocitrate dehydrogenase 3B
LRBA	4q31.3	int12	1.34	0.15	0.77	LPS-responsive vesicle trafficking
MK-STYX	7q11.23	int1	1.47	0.24	—	Map kinase phosphatase-like protein
NOL5A	20p13	2.5 kb up	1.49	0.24	2.20	Nucleolar protein 5A
PCCA	13q32.3	int5	2.72	1.46	1.47	Propionyl coenzyme A carboxylase
PFTK1	7q21.13	int9	2.55	0.39	2.24	PFTAIRE protein kinase 1 homolog cdc2
POT1	7q31.33	int1	1.31	0.08	1.09	Protection of telomeres 1
RFC1	4p14	int8	1.64	0.22	0.94	Replication factor C1
SLC2A5	1p36.23	ex8	1.30	0.22	1.42	Solute carrier family 2
SSR3#	3q25.31	10 kb dw	3.07	1.47	—	Signal sequence receptor, gamma
TBL1X	Xp22.22	int3	1.62	0.08	0.76	Transducin beta-like 1X protein
(b) Upregulation upon repression by EWS-FLI1-specific shRNA						
ATP1B1	1q24.2	10 kb up	2.35	0.19	0.28	Na^+/K^+ transporting ATPase beta 1
CDK7	5q13.2	int1	1.30	0.09	0.59	Cyclin-dependent kinase 7
FLJ21613	9q21.33	ex1	1.55	0.23	—	Amino-acid *N*-acetyltransferase subunit
KIAA1026#	1p36.13	int4	2.09	0.48	0.83	Kazrin
KIAA1361	17q11.2	int4	1.35	0.35	—	TAO1, STE 20-like Ser/Thr protein kinase
KIAA1432*	9p24.1	int2	2.20		—	Unknown
LIMS1#	2q12.3	ex1	1.27	0.13	0.75	LIM and senescent cell antigen-like domains 1
LIPA	10q23.2	int2	1.46	0.34	0.68	Lipase A, lysosomal acid, cholesterol esterase
MDH2	7q11.23	1 kb up	1.28	0.03	1.00	Malate dehydrogenase 2, NAD (mitochondrial)
NPY	7p15.1	10 kb up	3.29	2.61	0.94	Neuropeptide Y
NCAM1	11q23.1	int1	3.56	1.91	0.87	Neural cell adhesion molecule 1
PCLO	7q21.11	ex1	1.61	0.09	0.60	Piccolo (presynaptic cytomatrix protein)
RHOBTB3	5q15	int1	2.70	0.70	0.34	Rho-related BTB domain containing 3
TCF12	15q21.3	int2	1.39	0.28	1.82	Helix–loop–helix transcription factors 4
VGF	7q22	int1	2.07	0.27	0.58	Nerve growth factor, inducible

(c) EWS-FLI1 specific ChIP genes not classified by EWS-FLI1 specific RNAi

U133A and B	*Gene*	*Localization*		*ESFT/non-ESFT*	*Function*
		Chromosome	*Gene*	*Median ratio*	
Below threshold	ARNT2	15q25.1	int5	0.29	Aryl hydrocarbon receptor nuclear translocator 2
	BIA2	1q44	10 kb up	0.71	Unknown
	CDH13	16q23.3	int2	0.85	Cadherin 13
	CHL1	3p26.3	int2	0.66	Homolog of L1CAM cell adhesion molecule
	CNGB3	8q21.3	int13	—	Cyclic nucleotide-gated channel beta 3
	CYP4A11	1p33	ex1	0.89	Cytochrome *P*450-4A11
	DPP9	19p13.3	int2	—	Dipeptidylpeptidase 9
	EB-1	12q23.1	int1	—	E2a-Pbx1-associated protein
	FHIT	3p14.2	int4	0.73	Fragile histidine triad gene
	FLJ23049	3q26.2	int10	—	Unknown
	GRIA3	Xq25	int10	0.67+	Glutamate receptor. ionotrophic, AMPA 3
	HCMOGT-1	17p11.2	int3	—	Sperm antigen HCMOGT-1
	HESX1	3p14.3	1 kb up	0.75	Homeo box (expressed in ES cells) 1
	KCNAB1#	3q25.31	int5	1.42	Potassium voltage-gated channel beta1
	KIAA1680#	4q22.1	int7	—	Unknown
	LRP1B	2q22.1	int2	—	Low-density lipoprotein-related protein 1B
	LTF	3q21–q23	10 kb up	0.78	Lactotransferrin
	NR5A2	1q32.1	int6	0.91	Nuclear receptor subfamily 5A2
	PDE10A	6q27	int3	1.02	Phosphodiesterase 10A
	POPDC2	3q13.33	ex4	—	Popeye domain containing 2
	PTPRD	9p23	int7	1.04	Protein tyrosine phosphatase, receptor type, D
	RIT2	18q12.3	int4	1.78	Ras-like small GTPase RIBA
	XPR1	17p11.2	int2	—	Xenotropic and polytropic retrovirus receptor

Table 1 (*continued*)

U133A and B	*Gene*	*Localization*		*ESFT/non-ESFT*	*Function*
		Chromosome	*Gene*	*Median ratio*	
No change	ADCY1	7p13	int6	0.79	Adenylate cyclase 1
	ELKS	12p13.3	int16	0.61	Rab6-interacting protein 2
	FLJ32141	10p14	int1	—	Unknown
	GALNT10[#]	5q33.2	int2	0.74	*N*-acetylgalactosaminyltransferase 10
	HEY1	8q21.13	10 kb up	—	Hairy/enhancer-of-split related with YRPW motif 1
	ME1	6q14.2	int6	1.34	Breast cancer cytosolic NADP(+)-dependent malic enzyme
	NEK1	4q33	int13	0.76	NIMA (never in mitosis gene a)-related kinase 1
	NEO1	15q24.1	int10	0.75	Neogenin homolog 1
	NFIL3	9q22.31	int1	0.49	Nuclear factor, interleukin 3 regulated
	PAPPA	9q33.1	int12	1.82	Pregnancy-associated plasma protein-A
	PIP5K1B	9q21.11	int1	1.18	Phosphatidylinositol-4-phosphate 5-kinase 1beta
	PTPN4	2q14.2	int3	1.16	Protein tyrosine phosphatase, nonreceptor type 4
	PVT1[#]	8q24.21	int4	1.05	Pvt1 oncogene homolog, MYC activator
	TNFRSF10B	8p21.2	int1	1.29	TRAIL receptor type 2
	WWP2	16q22.1	int2	0.75[+]	Nedd-4-like ubiquitin-protein ligase
Not present on HG133A and B	AF424542	Xq21.1	int3	—	Rheumatoid retrotransposon L1
	AK057451	9q22.33	int2	—	Unknown
	AK090538	3q25.2	int1	—	Unknown
	AK091229	1q43	int2	—	Unknown
	AK091882	6q23.1	ex1	—	SAMD3
	AK092412	1p31	int7	—	Unknown
	AK094293	2q37.1	int1	—	Belongs to the ribonuclease ii (rnb) family
	AK094352	15q26.1	int2	—	Unknown
	AK094917	5q13.3	int1	—	SV2C ortholog of mouse synaptic vesicle glycoprotein 2a
	AL832144	3q26.32	int6	—	*N*-acetylated alpha-linked acidic peptidase 2
	BC028038	9q23	int6	—	Protein-tyrosine-phosphatase receptor type D
	BC038189	6q13	int2	—	Unknown
	BC041008	1q24.2	7 kb up	—	Unknown
	BC043355	2p16.1	int1	—	Unknown
	CCRL2	3p21.31	int1	1.02	Chemokine (C–C motif) receptor-like 2
	COP1	1q25.1	ex10	—	Constitutive photomorphogenic protein
	FLJ25799	6p22.3	ex6	—	Unknown
	FLJ32440	8q24.13	int4	—	Unknown
	GOR	8q21.2	int1	—	Exonuclease GOR
	GRID1	10q23.3	int2	—	Glutamate receptor, ionotropic, delta 1
	HS6ST3	13q32.1	int1	—	Heparansulfate 6-*O*-sulfotransferase 3
	LYRIC[#]	8q22.1	int2	1.21	Astrocyte-elevated gene-1
	Raptor	17q25.3	int1	—	TOR-scaffold protein with WD repeats
	SYTL5	Xp11.4	int2	—	Synaptotagmin-like 5
	TNRC6	16p12.1	int1	—	Trinucleotide repeat containing 6
	UVRAG	11q13.5	int11	1.00	UV radiation resistance-associated gene
	ZFYVE20	3p25.1	1 kb up	—	FYVE-finger-containing Rab5 effector protein Rabenosyn-5
	ZNF406	8q24.22	int8	—	Zinc-finger protein 406

Presentation of ChIP-derived genes (a) down- and (b) upregulated upon EWS-FLI1 knockdown in STA-ET-7.2 cells, and (c) of genes whose expression was either not affected by EWS-FLI1 modulation, not detectable or below threshold, or not represented on the Affymetrix microarray. Genes obtained more than once by ChIP are indicated (#). For EWS-FLI1 knockdown, three independent RNAi experiments were performed comparing shEF4 (targeting the fli1 3′ coding RNA portion) with shEF30 (mismatched control), shEF4 with empty vector control, and shEF22 (targeting the ews-fli1 type 2 fusion region) with shEF30 6 days after infection of STA-ET-7.2 cells. In (a) and (b), mean values (M) for the fold changes and standard deviations (s.d.) are shown, except for KIAA1432 present on the HG-U133B array only, which was tested only once (*). For each gene, the chromosomal assignment, the localization of ChIP-derived fragments in either the upstream region (up), downstream region (down), exon (ex) or intron (int) of the respective genes, and the putative function are indicated. Except for the genes not represented on the U95Av2 array (—), the expression of the individual genes in ESFT as compared to other small blue round cell tumors is presented as the median of signal intensities on Affymetrix HG-U95Av2 obtained from seven ESFT divided by the median of signal intensities for all non-ESFT samples including six osteosarcomas, eight neuroblastomas, and six clear-cell sarcomas. If a gene was represented by more than one probe set on the U95A-chip (+), mean values of all these probe sets were calculated first

levels decreased in EWS-FLI1 shRNA-treated cells, whereas the level of tgfβr2, which is repressed by EWS-FLI1, increased. Among the genes co-precipitating with EWS-FLI1-specific antibodies in our ChIP screen, 28 were not represented on the HG-U133A and B GeneChips, 23 lacked a detectable signal, and 15 were found to be present in STA-ET-7.2 cells but did not show any significant changes in gene expression upon

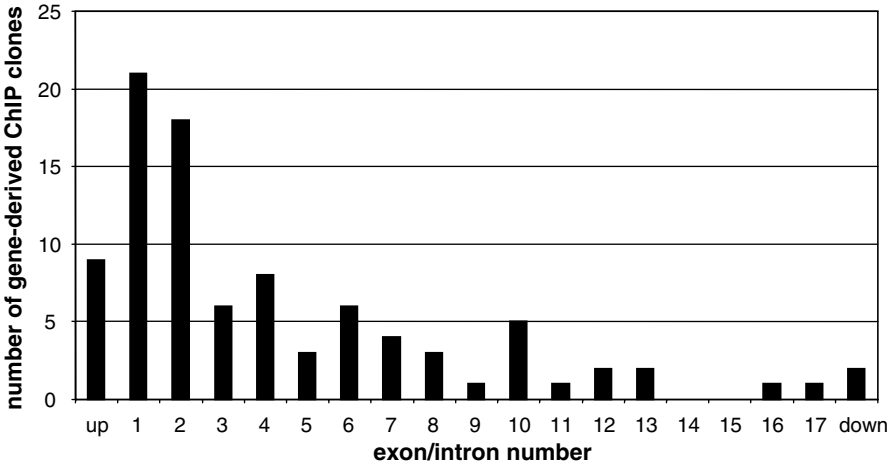

Figure 1 Assignment of EWS-FLI1-specific gene-derived ChIP clones to distinct gene regions. Figures on the *x*-axis represent exon/intron numbers; up, 10 kb of upstream region; down, 10 kb of downstream region. The number of EWS-FLI1-specific clones derived from the different gene regions is represented by the black bars. In all, 57% of fragments align to the upstream regions (12 fragments), and the first and second intron (27 and 18, respectively) of the genes

modulation of EWS-FLI1 (Table 1c). In contrast, 18 and 15 genes were found to be down- and upregulated by RNAi-mediated EWS-FLI1 suppression, respectively (Figure 3b and c). Although changes in the expression of these genes in individual experiments were low ranging from 1.3- to 5.9-fold, they were highly reproducible between the two different EWS-FLI1-specific shRNAs in the three independent experiments performed (Table 1a and b). Therefore, it is unlikely that the results obtained for target genes with low expression levels arise from background noise.

Similar results were obtained in ESFT cell lines TC252 and SK-N-MC, which express type 1 EWS-FLI1 in a germline EWS-positive background using shEF30 for RNAi (data not shown). Thus, at least 33 genes identified by our ChIP screen were found to be affected in expression by EWS-FLI1 in ESFT cells.

Expression pattern of putative direct EWS-FLI1 target genes in small round cell tumors

Previously, we monitored the expression pattern of seven ESFT cell lines in comparison to six osteosarcoma, eight neuroblastoma, and six clear-cell sarcoma of soft parts samples on Affymetrix HG-U95Av2 microarrays, which include probe sets for 58 of the genes isolated by ChIP (Schaefer *et al*., 2004). Of these genes, we found 16 and 12 down- and upregulated upon repression of EWS-FLI1, respectively (Table 1). Categorizing the expression values of each of these genes as either higher (median (ESFT)/median (non-ESFT) > 1) or lower (median (ESFT)/median (non-ESFT) < 1) in the ESFT *versus* the non-ESFT samples, we observed a significant correlation between genes generally activated in ESFT and genes which are downregulated upon EWS-FLI1 modulation and, *vice versa*, genes expressed at low level in ESFT and genes activated by EWS-FLI1 deprivation ($P = 0.0037$, χ^2 test).

Confirmation of in vivo *binding of EWS-FLI1 to candidate target genes by ChIP and PCR*

To confirm the association of EWS-FLI1 with chromatin at the cloned genomic regions, independent ChIP experiments followed by PCR with primers flanking the cloned sequences were performed for a subset of four candidate target genes whose expression changed upon EWS-FLI1 knockdown in STA-ET-7.2 cells to different extents. After two rounds of ChIP, amplification products were specifically obtained from either EWS or FLI1 antibody precipitations for the tested genes *ACCN1*, *MK-STYX*, *TCF12*, and *PFTK1*, providing further evidence for the direct *in vivo* interaction of EWS-FLI1 with these genes (Figure 4).

EWS-FLI1 binds to the MK-STYX *gene which is abundantly expressed in ESFT*

ETS proteins generally bind to the core consensus binding motif GGAA/T. This sequence was also found to be present in one to several copies in all the DNA fragments cloned from EWS-FLI-specific ChIP reactions. One of the isolated candidate EWS-FLI1 targets, MK-STYX, contained six canonical ETS recognition sequences within the precipitated genomic fragment from the first intron of the gene. MK-STYX encodes for a phosphatase-dead dual specificity phosphatase-like protein implicated in the regulation of MAP kinases (Wishart and Dixon, 1998) and therefore attracted our attention as a putative pleiotropic effector of EWS-FLI1. By real-time quantitative PCR, *MK-STYX* expression was consistently observed in all ESFT samples investigated (seven primary tumor samples and 10 unrelated ESFT cell lines) at a level of about 25-fold lower than beta 2 ($\beta 2$) microglobulin (mean difference in cycle threshold values 7.8, s.d. 1.8).

To further confirm direct binding of EWS-FLI1 to *MK-STYX*, the cloned 163 bp sequence was broken

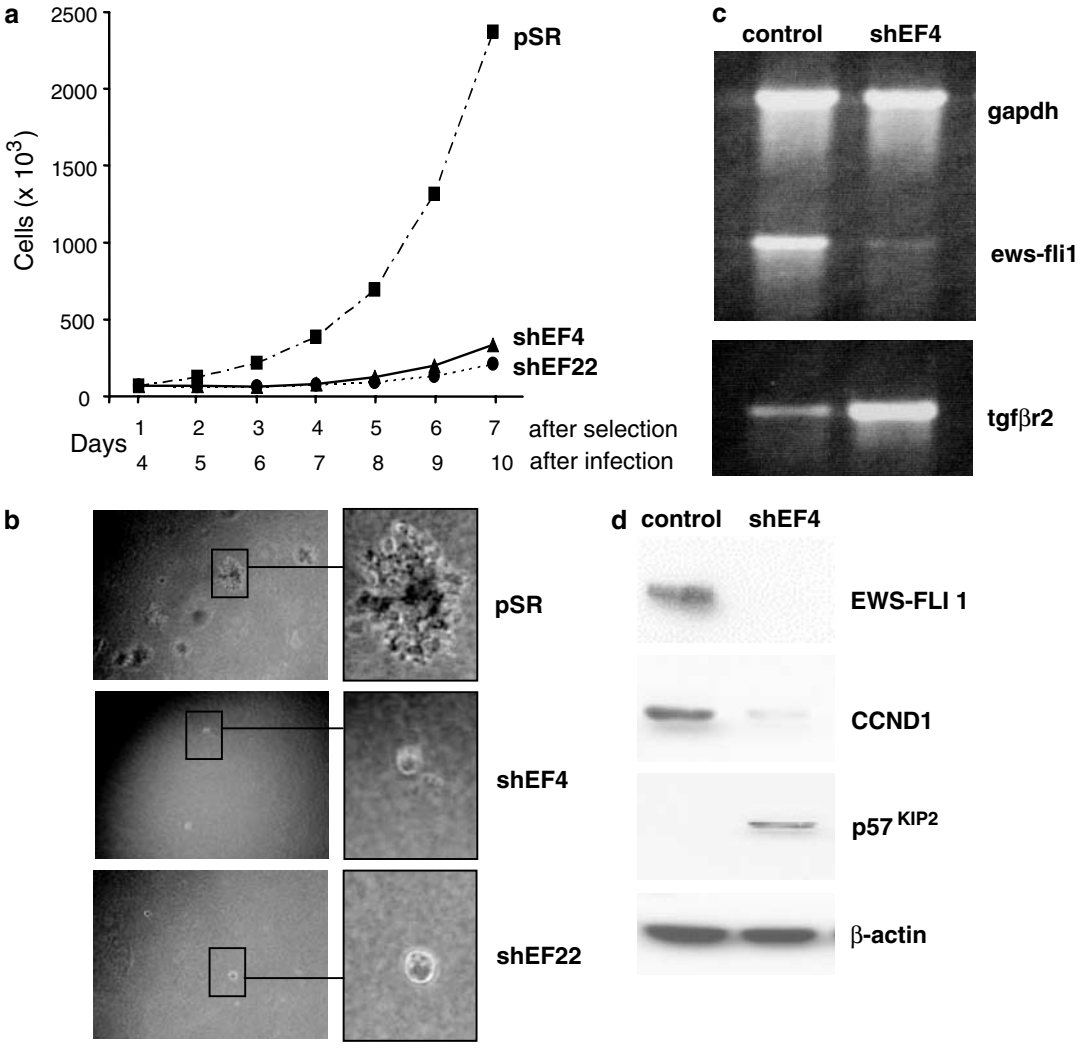

Figure 2 Effect of EWS-FLI1 suppression by RNAi on STA-ET-7.2 growth and the expression of known downstream genes. STA-ET-7.2 cells were infected with the indicated retroviral constructs and 1 day later subjected to puromycin selection for 2 days before cells were seeded for the determination of growth kinetics. (**a**) Monolayer growth on fibronectin-coated culture flasks. Cell numbers were determined by daily counts starting 1 day after an inoculum of 70 000 cells. (**b**) Soft-agar colony formation. A total of 200 000 cells were plated into soft agar at the same time as for the assessment of monolayer growth and the number and morphology of colonies was regularly monitored. Shown are pictures of representative fields obtained after 8 days (11 days after infection) at 10-fold magnification (left) and a close-up of cells at 20-fold magnification (right). (**c**) RT–PCR of STA-ET-7.2 cells 6 days after infection with shEF4 and a control shRNA construct. Multiplex PCR with primers for the amplification of ews-fli1 and the control transcript gapdh show a significant decrease of ews-fli1 mRNA in cells infected with the retroviral construct shEF4. As a consequence of ews-fli1 suppression, tgfβr2 mRNA levels increased. (**d**) Western blot demonstrating the effect of EWS-FLI1 suppression on CCND1 and p57^{KIP2} protein expression. β-actin is shown as a loading control

down into three subfragments, MK1, MK2, and MK3, each containing pairs of the ETS recognition motif (Figure 5a), which were subjected to electromobility shift assays (EMSAs) with EWS-FLI1. A *TGFβR2* promoter fragment was used as a positive control. Using recombinant EWS-FLI1 protein alone, no EWS-FLI1-specific protein–DNA complexes were detectable. The addition of an FLI1 antibody greatly stimulated binding of EWS-FLI1 to the *TGFβR2* promoter and the MK2 fragment (Figure 5b). Similar results were obtained for recombinant factor Xa-digested GST-EWS-FLI1 protein and EWS-FLI1 immunopurified from STA-ET-7.2 and SK-N-MC cells (Figure 5c). The need for antibody binding to allow protein–DNA interaction *in vitro* may reflect the requirement for cellular protein interactions absent from the *in vitro* reaction (Staal *et al*., 1996). Unlabeled double-stranded MK2 and TGFβR2 oligonucleotides efficiently competed for complex formation with EWS-FLI1, while an unrelated competitor (HRAS) did not, confirming the specificity of the MK2 complexes for EWS-FLI1 (Figure 5c and d). Mutating the second GGAA motif (mk2-2) of fragment MK2 (MK2-2m competitor) significantly reduced its ability to compete for EWS-FLI1 binding, whereas the MK2-1m fragment with a mutation of the first motif mk2-1 was similarly effective in competition as wild-type MK2,

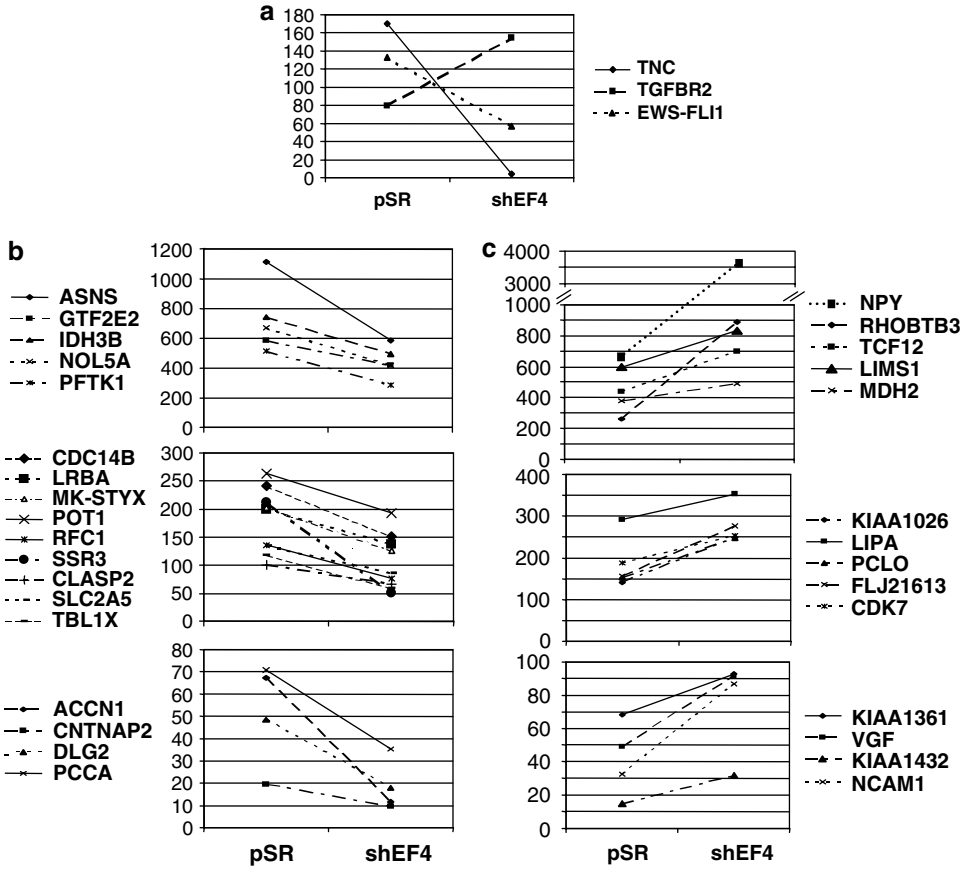

Figure 3 Changes in expression of known and putative EWS-FLI1 target genes assessed by GeneChip analysis of EWS-FLI1 RNAi-suppressed STA-ET-7.2 cells. Alterations in the transcriptome were followed on Affymetrix HG-U133A and B microarrays after suppression of EWS-FLI1 by RNAi. Three independent experiments have been performed comparing shEF4- or shEF22-suppressed STA-ET-7.2 cells with mismatch (shEF30) and empty control vector-treated cells 6 days after retroviral infection. Results of one representative experiment comparing shEF4 to empty vector control (pSR) are shown. Expression levels are presented as signal intensities on the microarray. For validation of the approach, (**a**) presents the decrease in ews-fli1 RNA paralleled by the expected increase in tgfβr2 and decrease in tnc RNA levels. Of the 99 genes, 33 isolated by the ChIP approach showed altered expression upon modulation of EWS-FLI1 as shown in detail in (**b**) for downregulated and in (**c**) for induced genes. Genes with high expression values are depicted at the top, genes with medium expression levels in the middle, and genes with low expression values at the bottom. Mean values and standard deviations for all experiments performed are presented in Table 1a and b

identifying mk2-2 as the binding site for EWS-FLI1 (Figure 5d). EMSAs using the two mutated fragments MK2-1m and MK2-2m as probes confirmed the requirement for an intact mk2-2 site, since mutation of mk2-2 but not of mk2-1 significantly reduced binding of EWS-FLI1 to DNA. These results confirm that a single ETS binding motif is sufficient for binding of EWS-FLI1.

EWS-FLI1 regulates the expression of MK-STYX in vivo

Quantification of *MK-STYX* expression in the absence or presence of EWS-FLI1-specific shRNA by real-time PCR confirmed the microarray results. When *EWS-FLI1* expression was suppressed by 86%, tgfβr2 levels increased sevenfold in STA-ET-7.2 cells. Concomitantly, an 80% reduction in mk-styx RNA was revealed (Figure 6a). Similar results were obtained in the ESFT cell line SK-N-MC (data not shown).

To test directly the functional consequences of EWS-FLI1 interaction with *MK-STYX*, the 163 bp genomic fragment isolated by ChIP was used in reporter gene assays in the neuroblastoma cell line SJ-NB-7 (Figure 6b). In the presence of cotransfected EWS-FLI1, a dose-dependent induction of luciferase activity was obtained. No activation was observed with the empty vector control (not shown). Mutation of the mk2-2 ets binding site within the 163 bp MK-STYX genomic fragment greatly reduced reporter gene activity confirming the essential role of EWS-FLI1 binding to mk2-2 in the transcriptional activation of the gene. Reporter gene activities obtained in the presence of transfected EWS-FLI1 in non-ESFT cells may lead to an underestimation of the transcriptional potential of a regulatory element, since ectopic EWS-FLI1 expression is known to result in various levels of apoptosis in heterologous cell types. We therefore incubated EWS-FLI1-transfected SJ-NB-7 cells in the presence of the general caspase inhibitor Z-Val-Ala-DL-Asp-fluoro-

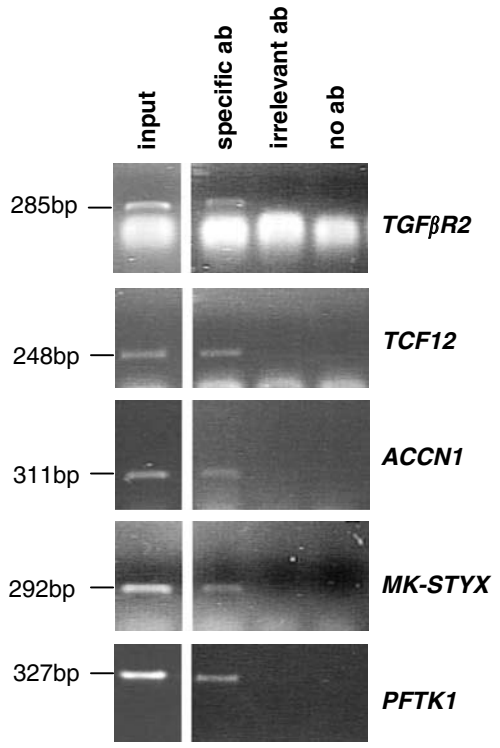

Figure 4 Confirmation of the *in vivo* interaction between EWS-FLI1 and four candidate target genes in an independent ChIP experiment. PCR on ChIP products from four genes, one upregulated (*TCF12*) and three downregulated (*ACCN1*, *MK-STYX*, and *PFTK1*) to different extents upon knock down of EWS-FLI1, obtained by two successive rounds of immunoprecipitation from STA-ET-7.2 cells. The *TGFβR2* gene promoter, which is downregulated by EWS-FLI1, served as a control for the ChIP reactions. Amplification products were obtained when EWS-FLI1-specific antibodies (C19 or 139/2) but not irrelevant (anti-KAI) or no antibody were used. Input, PCR from isolated chromatin before precipitation

methyl ketone (z-VAD.fmk), resulting in a further threefold increase in reporter gene activity (Figure 6b, lower panel). *MK-STYX* promoter-driven luciferase expression was also increased upon forced expression of ectopic EWS-FLI1 within the ESFT context (STA-ET-7.2, Figure 6c). Upon cotransfection of shEF4 to counteract EWS-FLI1 expression, but not of the mismatched shEF4M control vector, reporter induction was reversed. ShEF4, but not shEF4M, also suppressed basal reporter gene activity in STA-ET-7.2 cells, compatible with endogenous EWS-FLI1 being responsible for constitutive *MK-STYX* promoter activity in ESFT cells. These results provide functional confirmation for successful isolation of direct EWS-FLI1 target genes by our dual ChIP approach.

Discussion

Ectopic expression models for the study of transcription factor function in heterologous cells harbor a major disadvantage: they do not account for the authentic cellular context that may affect accessibility of chromatin to the factor and influence selection and regulation of potential targets. In addition, target gene regulation may depend on the level of expression of the regulatory protein of interest. We therefore approached the problem of target identification for the ESFT-specific translocation product EWS-FLI1 by a combination of two methods, ChIP and RNAi, targeting endogenous EWS-FLI1 directly in ESFT cells. The list of candidate EWS-FLI1 binding genes obtained has to be considered as incomplete since none of the previously established target genes was obtained and out of 99 genes cloned only nine genes were hit more than once. Of this list, 55 genes are represented on the HG-U95Av2 microarray used in a study of inducible ectopic EWS-FLI1 expression in hTERT-immortalized human fibroblasts (Lessnick *et al*., 2002). In this transgenic model system, 13 and eight genes were up- and downregulated, respectively, but only 12 genes overlapped with the set of 33 genes affected by modulation of EWS-FLI1 in ESFT. Of these, four genes (*ACCN1*, *PCCA*, *PFTK1*, *SLC2A2*) showed upregulation upon EWS-FLI1 induction in the fibroblast model and downregulation upon EWS-FLI1 suppression in ESFT cells.

In the RNAi experiments targeting EWS-FLI1 in ESFT cells, the fold change in expression of EWS-FLI1-specific candidate genes cloned from ChIP products was low but highly reproducible, while the genes most affected by EWS-FLI1 suppression showed an up to 200-fold change in microarray analyses (not shown). In a biological system, a slight change in the expression of a gene upstream of a signal transduction cascade may lead to a multiplication of the signal in the downstream hierarchy. Trisomy of chromosome 8, which appeared to be enriched in putative EWS-FLI1 target genes, occurs with a frequency of about 50% in ESFT and may be envisaged as a mechanism to further increase the dosage of EWS-FLI1-specific genes (Hattinger *et al*., 2002).

It is noteworthy that only 12% of ChIP clones were derived from the upstream regulatory regions, while 45% derived from the first two introns. Although there are examples for *bona fide* transcription factors, which bind to their targets preferentially in introns, this finding may as well point to functions distinct from mere transcriptional regulation. Increasing evidence suggests that pre-mRNA splicing takes place cotranscriptionally. EWS fusion proteins have been demonstrated to alter splice site selection in experimental systems and to interfere with YB-1-mediated splicing (Chansky *et al*., 2001; Ohkura *et al*., 2002). YB-1 links transcription to RNA processing, being normally recruited to the RNA polymerase II complex via interaction with germline EWS or its close relative TLS. In ESFT cells that express EWS-FLI1, this linkage was found to be defective. For the ETS transcription factor SPI1/PU1, which interacts with TLS abrogating its function in splice site selection as well (Hallier *et al*., 1998), evidence was obtained that the splicing effect depends on the ETS DNA-binding domain together with the transactivation domain implicating a role for direct DNA binding in this

process (Delva *et al*., 2004). Intriguingly, many of the candidate target genes of EWS-FLI1 identified by our ChIP approach are known to be expressed in a multitude of differently initiated and/or spliced variants in different tissues. Therefore, it will be interesting to study the isoform expression pattern for each individual putative EWS-FLI1 target, whose overall expression was only moderately or not affected in response to EWS-FLI1 suppression.

Among the genes that showed an ESFT-specific expression pattern when compared to other small blue round cell tumors of childhood is the tumor suppressor *DLG2*, a membrane-associated guanylate kinase homologue that interacts with protein 4.1 in epithelial cells and in the presynaptic neuron. Notably, several other genes arising from our EWS-FLI1-specific ChIP screen including *PCLO*, *NCAM1*, *NPY* and *CNTNAP2* play roles in this cell type as well. Altogether, expression of at least one-fifth of genes precipitating with EWS-FLI1-specific antibodies has been described as being associated with neural tissue. This finding is intriguing since ESFT show limited neural differentiation, which has previously been taken as an argument for neural histogenesis of the disease. However, the partial neural differentiation potential of ESFT may be linked to EWS-FLI1-mediated deregulation of neural target genes.

We focused on *MK-STYX* as an example for a gene isolated by ChIP and only moderately affected by EWS-FLI1-directed RNAi to demonstrate binding of and regulation by EWS-FLI1. Interestingly, the site recognized by EWS-FLI1 very closely resembled that of the *TGFβR2* gene, a previously confirmed EWS-FLI1

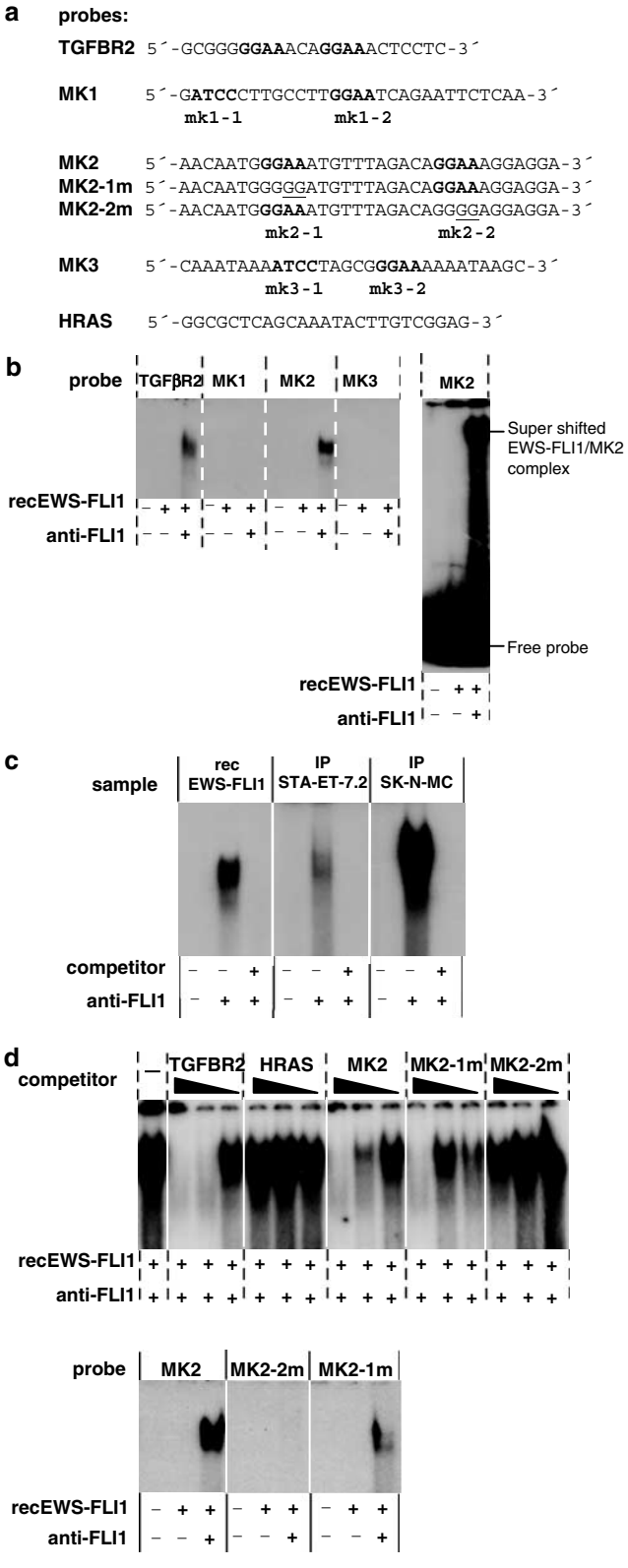

Figure 5 *In vitro* binding of EWS-FLI1 to putative ETS core consensus sites in the first intron of *MK-STYX*. (**a**) Probes used for EMSA with recombinant EWS-FLI1. A *TGFβR2* promoter fragment and a fragment of the first intron of *HRAS* were used as positive and negative controls, respectively. Three probes (MK1, MK2, MK3) containing the six putative ETS consensus binding sites mk1-1, mk1-2, mk2-1, mk2-2, mk3-1, and mk3-2 (in bold) were generated to delineate the region of interaction with EWS-FLI1 within the 163 bp fragment from the first intron of the *MK-STYX* gene cloned by the dual ChIP approach. In probes MK2-1m and MK2-2m, the putative ETS binding motifs mk2-1 and mk2-2 were mutated from GGAA to GGGG (underlined). (**b**) EMSA with recombinant EWS-FLI1 (recEWS-FLI1) and TGFβR2, MK1, MK2, and MK3 as probes in the absence and presence of FLI1-specific monoclonal antibody Hyb7.3 demonstrating binding of MK2 to EWS-FLI1 but only in the presence of FLI1 antibody. The right panel presents a slightly compressed view of the whole gel demonstrating the absence of any protein–DNA complex in the absence of FLI1 antibody. (**c**) EMSA with endogenous EWS-FLI1 immunopurified from STA-ET-7.2 and SK-N-MC cells (IP) as compared to recEWS-FLI1 using MK2 as radioactively labeled probe in the absence or presence of a 10-fold excess of cold-specific competitor and FLI1 antibody. In the presence of FLI1 antibody, endogenous EWS-FLI1 from ESFT cells formed specific complexes with MK2 similar to recEWS-FLI1. A slightly slower migration of complexes with ESFT-expressed EWS-FLI1 may be caused by post-translational modifications absent in recEWS-FLI1 (data not shown). (**d**) Upper panel: Binding of recEWS-FLI1 to MK2 in the presence of FLI antibody and a 100-, 10-, and twofold excess of cold probes TGFβR2, HRAS, MK2, MK2-1m, or MK2-2m as competitors. Only TGFβR2, MK2, and MK2-1m were capable of efficiently competing for complex formation with EWS-FLI1 suggesting mk2-2 as binding site for EWS-FLI1. Lower panel: EMSA using MK2 and mutant MK2-1m and MK2-2m probes. Only MK2 and MK2-1m formed complexes with EWS-FLI1 compatible with mk2-2 being responsible for binding of EWS-FLI1 to MK2

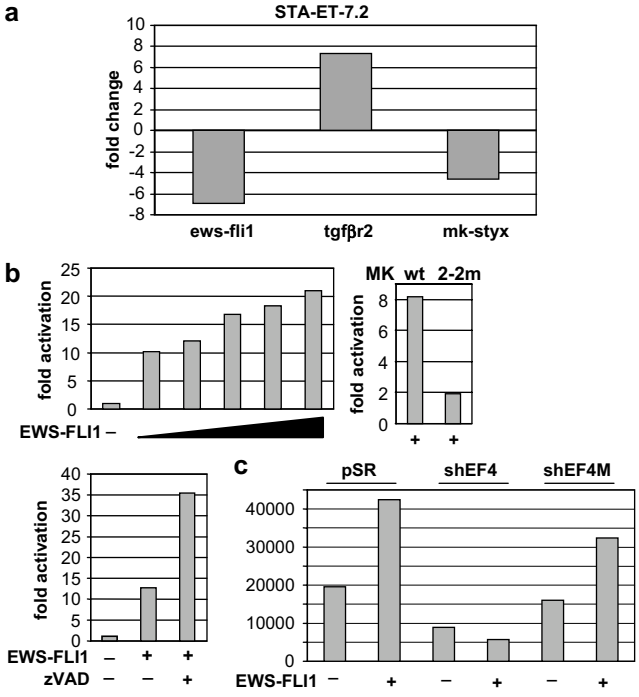

Figure 6 Regulation of *MK-STYX* by EWS-FLI1. (**a**) Fold changes in *EWS-FLI1*, *TGFβR2*, and *MK-STYX* expression in STA-ET-7.2 cells as measured by real-time quantitative PCR 6 days after the introduction of retroviral shRNA expression vectors against ews-fli1. Values were normalized against $\beta 2$ microglobulin, which is unaffected by EWS-FLI1, and the fold change between shEF4-suppressed cells and control-infected cells was calculated. (**b**) Reporter gene assays in SJ-Nb7 cells demonstrating specific activation of the MK-STYX promoter by ectopically expressed EWS-FLI. Transfections were performed in triplicate and mean values are presented as fold changes compared to the empty expression vector control in representative experiments. Left panel: Dose-dependent activation of *MK-STYX* fragment-driven luciferase expression by EWS-FLI1. A measure of 50 ng of the reporter vector pGL3-promotor-MK-STYX, containing the 163 bp genomic fragment isolated by ChIP, was transfected with increasing amounts (12.5, 25, 50, 75, and 100 ng) of EWS-FLI1 expression vector supplemented with empty expression vector to a final of 150 ng transfected DNA. Middle panel: Since EWS-FLI1 may be toxic at high concentrations, the caspase inhibitor z-VAD.fmk was added to the highest concentration of EWS-FLI1 in an additional experiment to prevent apoptosis of transfected cells. Right panel: EWS-FLI1-driven reporter gene activation from the 163 bp genomic MK-STYX fragment in the absence (wt) and presence of an mk2-2 mutation (2-2m). A measure of 50 ng of reporter vector was cotransfected with 100 ng EWS-FLI expression vector. (**c**) Reporter gene activity of pGL3-promoter-MK-STYX in STA-ET-7.2 cells in the absence or presence of ectopically expressed EWS-FLI1 (indicated below the figure) and either empty pSR or shEF4 or mismatched shEF4M expression vectors (indicated on top). Transfections were performed in triplicate and mean values with standard deviation of light units are given. Repression of endogenous (compare third to first column) and ectopically expressed EWS-FLI1 (compare fourth to second column) by shEF4-mediated RNAi significantly reduced reporter activity, while the mismatched control vector shEF4M did not (compare fifth to first and sixth to second column)

target, indicating a preference for the sequence ACAGGAAA. MK-STYX belongs to the family of MAP kinase phosphatases but lacks enzymatic activity due to an amino-acid exchange in the active center of the protein. The actual function of STYX proteins is not known. It is suggested that they bind to phosphorylated kinases, thereby preventing dephosphorylation by active phosphatases keeping the kinases in an active state. It will therefore be of great interest to study the influence of EWS-FLI1 on the MAP kinase pathway in ESFT in more detail. However, STYX proteins may also serve alternative functions by complexing with other phosphorylated proteins such as CRHSP-24, an RNA-binding protein implicated in translational repression of histone mRNAs and involved in differentiation of spermatids (Wishart and Dixon, 2002). So far, our results for *MK-STYX* provide proof of principle for the relevance of a combined ChIP/RNAi approach to the identification of EWS-FLI1 target genes in its authentic cellular context. However, it will be necessary to validate each individual gene isolated from our screen for consistency of the presence or absence of expression in a panel of ESFT and further confirm binding of and regulation by EWS-FLI1 independently in order to determine those genes which may be of general importance to ESFT pathogenesis. So far, our results lay the basis for detailed functional studies downstream of EWS-FLI1 to unravel the pathogenetic processes resulting in ESFT development.

Materials and methods

Chromatin immunoprecipitation

STA-ET-7.2 cells were grown on fibronectin-coated plastics. A total of 8×10^7 cells were harvested by trypsin/EDTA treatment and resuspended in 30 ml growth medium. After crosslinking for 15 min in 1% formaldehyde, cells were washed twice with ice-cold phosphate-buffered saline containing protease inhibitors (complete tablets; Roche Diagnostics, Vienna, Austria). Cells were lysed for 10 min on ice in 400 μl SDS lysis buffer containing protease inhibitors. Lysates were sonicated on ice to give chromatin fragments of approximately 200–1000 bp, and centrifuged and diluted to 1 ml with ChIP dilution buffer (0.01% SDS, 1.1% Triton X-100, 1.2 mM EDTA, 16.7 mM Tris-HCl, pH 8.1, 167 mM NaCl). Preclearing of lysates was performed for 30 min at 4°C using 100 μl Protein G Sepharose™ 4 Fast Flow (Amersham Biosciences, Vienna, Austria) blocked with tRNA and bovine serum albumin. Subsequently, the sepharose beads were pelleted and 100 μl protein G sepharose preincubated with 5 μl rabbit polyclonal Fli-1 C-19 or 5 μl KAI-1 C-16 antibodies (both from Santa Cruz Biotechnology, Santa Cruz, CA, USA), or no antibody was added to the supernatant. First-round ChIP was performed overnight at 4°C on a rotating wheel. Immunoprecipitates were washed once in low salt buffer (0.1% SDS, 1% Triton X-100, 2 mM EDTA, 20 mM Tris-HCl, pH 8.1, 150 mM NaCl), once in high salt buffer (0.1% SDS, 1% Triton X-100, 2 mM EDTA, 20 mM Tris-HCl, pH 8.1, 500 mM NaCl), and twice in TE. Chromatin complexes were eluted from the protein G sepharose using 200 μl elution buffer (1% SDS, 0.1 M $NaHCO_3$) for 30 min under agitation. For each antibody, an aliquot of 15 μl of the ChIP reaction was mixed with 2 × SDS sample buffer for SDS–PAGE analysis, and the efficiency and specificity of the ChIP reaction was monitored on Western blots probed with FLI1 C19 antibody (not shown). The major fraction of the eluates were diluted

with ChIP dilution buffer and split into four aliquots, which were subsequently incubated at 4°C overnight with protein G sepharose-bound antibodies FLI1 C-19, EWS 139/2 (a kind gift from CT Denny, UCLA, Los Angeles, Ca USA), KAI-1 C-16 and no antibody for a second round of precipitation. After repeated washings in low and high salt buffers and TE, precipitated chromatin was eluted into 150 μl elution buffer. The eluates were incubated with 8 μl of 5 M NaCl at 65°C for 5 h, followed by proteinase K and RNaseA treatment in the presence of 4 μl of 0.5 M EDTA and 8 μl 1 M Tris-HCl (pH 6.5) at 45°C for 30 min to reverse the crosslinks and release the genomic DNA from immunoprecipitated chromatin complexes. The DNA was recovered by phenol/chloroform extraction and ethanol precipitation with glycogen as an inert carrier overnight at −20°C. DNA pellets were dissolved in 40 μl sterile H_2O. To validate the efficiency of the dual ChIP reaction, PCR for the presence of *TGFβR2* promoter sequences, an established direct target of EWS-FLI1, was performed after the second round of precipitation and resulted in specific signals exclusively in the samples obtained by the EWS-FLI1-specific antibodies (not shown). No signals were obtained using primers for an irrelevant gene (β2 microglobulin). This result served as a surrogate for the enrichment of EWS-FLI1-specific genomic sequences in the precipitated protein–DNA complexes. Further analysis of EWS-FLI1-bound DNA was performed on pooled second-round ChIP samples.

Shot-gun cloning of chromatin-associated DNA

DNA precipitated by ChIP was digested with *Sau3*AI (Amersham Biosciences, Vienna, Austria) in 30 μl overnight at 37°C. Water was added to a total volume of 200 μl before phenol/chloroform extraction. After the addition of 4 ng of *Bam*H1 digested and dephosphorylated pBluescript (Stratagene, Amsterdam, The Netherlands), the DNA was precipitated and ligated to the vector using T4 DNA ligase (Promega, Mannheim, Germany) overnight and transformed into *Escherichia coli* JM109 cells (Promega). Inserts of a size larger than 150 bp were sequenced.

PCR on ChIP products

PCR reactions were performed using DyNAZyme™ II DNA polymerase (Finnzymes, Espoo, Finnland). As template, 1 μl of chromatin immunoprecipitated DNA or input DNA was used. Amplification was performed with 40 cycles consisting of denaturation at 95°C, annealing at 60°C, and extension at 72°C for 30 s each. Forward and reverse primers for *TGFβR2* were GTGTGGGAGGGCGGTGAGGGGC and GAGGGA AGCTGCACAGGAGTCCGGC, for *ACCN1* CCTCTCCTT CTCTGTCTGATC and GCAGCTCAGGCCCTATCATC, for *TCF12* CCAGTTGCCTGAAGTATCTATC and CTCAC TCATTAATTAATCTCCTGC, for *PFTK1* 5′-CAAGCAG GAGGTAGTTTAAGGC and GGCAGTTGCCTCAGATT CTCAC, and for *MK-STYX* GAACATTCAACTCCAGAG GAGG and CTCTCAGTTACAAGACAGAGGAG.

RNA interference

Suppression of EWS-FLI1 in ESFT cells by RNAi was accomplished using a pSUPER-based retroviral shRNA expression system as described in (Brummelkamp *et al*., 2002). Two vectors were constructed targeting the sequence CACCCACGUGCCUUCACAC in the FLI1 3′ coding region (EF4), and GCUACGGGCAGCAGAGUUC overlapping the fusion region of type 2 ews-fli1 RNA (EF22). For EF4, a mismatched control EF4M was designed (CACCCACGGUC CUUCACAC). To target the fusion region of type 1 ews-fli1, a previously published siRNA sequence was used (Dohjima *et al*., 2003) (designated EF30 in the context of this manuscript), which also served as a mismatched control in experiments targeting type 2 ews-fli1 RNA. siRNA sequences were converted to shRNA expression cassettes, cloned into the retroviral self-inactivating virus pSuperRetro (pSR) (a gift from R Agami, The Netherlands Cancer Institute, Amsterdam, The Netherlands), and amphotropic retroviral stocks were prepared from the Phoenix packaging cell line Pro-Pak-A.52 (ATCC, Rockville, MD, USA) 2 days after transfection with LipofectAMINE Plus reagent (Invitrogen, Groningen, The Netherlands). STA-ET-7.2 cells were infected with 1 : 3 diluted supernatant of the packaging cell line and subjected to puromycin selection 1 day after infection. Cells were either maintained as monolayer cultures or plated into 0.35% soft agar 2 days after the start of puromycin selection. Multiplex PCR for ews-fli1 and gapdh RNA expression was performed with ews-fli1 primers TCCTACAGCCAAGCTCCAAGTC and ACTCCCCGTTGGTCCCCTCC and gapdh primers TGAAGGTCGGAGTCAACGGATTTGGT and CATGTG GGCCATGAGGTCCACCAC in a competitive PCR reaction consisting of 25–35 amplification cycles of 30 s at 94°C, 1 min at 65°C, and 1 min at 72°C. Semiquantitative RT–PCR for induction of *tgfβr2* expression was performed with primers TTGCTCACCTCCACAGTGATC and GAGCCGTCTTCA GGAATCTTC in 30 cycles of 1 min at 95°C, 1 min at 58°C, and 2 min at 72°C.

Gene expression profiling

Changes in gene expression profiles of ESFT cells upon knock down of EWS-FLI1 by RNAi were followed on Affymetrix HG-U133A and B GeneChips® (Affymetrix Inc., Santa Clara, CA, USA). cRNA target synthesis and GeneChip® hybridizations, washing and staining steps, scanning, and data analysis (MAS 5.0, MicroDB 3.0, DMT 3.0) were carried out according to standard protocols recommended by the manufacturer (Affymetrix Inc., Santa Clara, CA, USA) and performed by the local Affymetrix Service Provider (VBC-Genomics Research GmbH, Vienna, Austria). Differences in signal intensities on Affymetrix chips between control-infected and shEF-suppressed ESFT cells were considered as representative for altered gene expression only if detection *P*-values for present calls were below 0.05 in all three experiments. Gene expression was considered induced or repressed if change in *P*-values were <0.006 and >0.994, respectively, in all three comparative RNAi experiments performed.

To correlate this set of up- and downregulated genes with expression data obtained by the microarray-based comparison of ESFT *versus* non-ESFT cell lines (HG-U95Av2, Affymetrix Inc., Santa Clara, CA, USA; Schaefer *et al*., 2004), the data set of the latter study was also dichotomized. For this purpose, the median expression value of seven ESFT cell lines was divided by the median expression of six osteosarcoma, six clear-cell sarcoma of soft parts, and eight neuroblastoma samples. Genes showing ratios greater than 1.00 were considered 'specifically overexpressed in ESFT', while values less than 1.00 define genes 'specifically underexpressed in ESFT'. If a gene was represented by more than one probe set on the U95A-chip mean values across these probe sets were calculated first. The overall correlation between sets of genes either suppressed by EWS-FLI1 silencing and overexpressed in ESFT or induced by EWS-FLI1 silencing and underexpressed in ESFT was calculated using the χ^2 test.

Electromobility shift assay

Recombinant GST-EWS-FLI1 fusion protein and cellular extracts were generated as described earlier (Spahn *et al*., 2002). For immunopurification of endogenous EWS-FLI1, cell extracts were prepared from 3×10^7 cells (SK-N-MC and STA-ET-7.2). FLI1 antibody (15 μl) (Santa Cruz Biotech., Santa Cruz, CA, USA) was chemically crosslinked to 100 μl sheep anti-rabbit-coupled magnetic dynabeads® (Dynal Biotech ASA, Oslo, Norway) using dimethyl pimelinediimidate dihydrochloride (Sigma-Aldrich, St Louis, MI, USA) as a cross-linking agent. Immunoprecipitations were carried out overnight at 4°C, and the precipitate was washed five times with lysis buffer. EWS-FLI1 was eluted into 40 μl of 100 mM glycine/HCl (pH 2) and the eluate was neutralized with 1 M Tris/HCl (pH 9), of which 10–20 μl were used for EMSA.

A measure of 10 ng of Factor Xa-digested recombinant EWS-FLI1 or immunopurified EWS-FLI1 was incubated with 15 000 c.p.m. of ^{32}P-labeled double-stranded oligonucleotides in 20 μl binding buffer (20 mM HEPES, pH 7, 2.6 mM $MgCl_2$, 5% glycerol, 40 mM KCl, 100 μM EDTA, 0.1% NP-40) for 30 min at room temperature. For supershifts, 3 μl of undiluted FLI1 Hyb7.3 hybridoma supernatant was used. Competition experiments were performed in the presence of a 100-fold excess of unlabeled double-stranded oligonucleotides, which were added to the reaction 15 min prior to the labeled probe. Samples were separated on a 5% nondenaturing PAA gel in 0.5 × TBE at 4°C. The sequences for the *TGFβR2* and *MK-STYX* probes are presented in Figure 6a.

Real-time PCR

Reactions were set up in a total volume of 25 μl containing 12.5 μl 2 × Universal Master Mix, including ROX-reference dye and uracil *N*′-glycosylase (Applied Biosystems, Vienna, Austria) and AmpliTaq Gold DNA polymerase (Perkin-Elmer, Boston, MA, USA), 300 nM (*TGFβR2*) or 900 nM (*EWS-FLI1, MK-STYX*) of primers, 100 nM (*MK-STYX*) or 200 nM (*EWS-FLI1*, *TGFβR2*) of TaqMan probe, and 1 μl of cDNA template. The mixtures were prepared in 96-well optical microtiter plates and amplified on the ABI 7700 or 7900 Sequence Detection System using the following cycling parameters: 2 min at 50°C, 10 min at 95°C, and 50 cycles of 15 s at 95°C and 60 s at 60°C. Primer and probe sequences were as follows: for *EWS-FLI1* CAGCCAAGCTCCAAGTCAA TATAG, AGGTTGTATTATAGGCCAGCAGTGA, and 6-FAM-CTCCTACCAGCTATTCCTCTACACAGCCGACTT AMRA; for *TGFβR2* TCGTCCTGTGGACGCGTAT, TG TCAGTGACTATCATGTCGTTATTAACC, and 6-FAM AGCACGATCCCACCGCACGTTC-TAMRA; for *MK-ST YX*CACTGCCCTTCGAGTGAAGAA, GTTGTTATCATA CACCACGCAGTACTT, and 6-FAM-TGAATATCTTCTC CCGGAGTCTGTGGACC-TAMRA; and for *β2M* TGAG TATGCCTGCCGTGTGA, ACTCATACACAACTTTCAG CAGCTTAC, and 6-FAM-CCATGTGACTTTGTCACAGC CCAAGATAGTT-TAMRA.

Reporter gene assays

Wild-type and mutant 163 bp MK-STYX fragments were cloned into pGL3-promotor vector (Promega, Mannheim, Germany). An MK-STYX genomic fragment carrying a mutant mk2-2 site was assembled from two overlapping fragments, each generated by PCR combining MK2-2m sequences (Figure 5a) as either reverse or forward primer with forward and reverse primers from the end of the 163 bp MK-STYX fragment including *Kpn*1 and *Xho*1 restriction sites (TACGGTACCGATCCCTTGCCTTGGAATCAG and CCGCTCGAGGATCTATTCACTGTCCCCTGA). Neuroblastoma cells SJ-NB-7 (provided by T Look, St Jude Children's Research Hospital, Memphis, TN, USA) were transfected in 24-well plates in quadruplicates with 50 ng pGL3-promotor-MK-STYX wild-type or mutant vectors and 150 ng of empty pCMV-FM plus pCMV-FM-EWS-FLI1 expression vectors (Spahn *et al*., 2002) in different ratios as indicated and incubated in the absence or presence of 0.2 mM of the general caspase inhibitor z-VAD.fmk (Bachem, Bubendorf, Switzerland) for 24 h. For shRNA repression of EWS-FLI1-mediated MK-STYX activation, STA-ET-7.2 cells were transfected with 25 ng of reporter vector pGL3-promotor-MK-STYX, 25 ng of empty pCMV-FM vector or pCMV-FM-EWS-FLI1 expression vector, and 200 ng of pSR, shEF4, or the mismatch control shEF4M in quadruplicates. In all reporter gene experiments, 50 ng of an EGFP expression vector was included into one of the quadruplicates to monitor transfection efficiencies by flow cytometry. The remaining triplicates were measured for luciferase activity using Bright-Glo Luciferase Assay System (Promega, Madison, USA) 24 h after transfection.

Acknowledgements
We thank Franz Watzinger and Lenka Baskova for help with real-time PCR. This study was supported in part by Grants 14299GEN and 16067-B04 from the Austrian Science Fund, by Grant GZ 200.071/3-VI/2a/2002 'GEN-AU Child' from the Austrian Federal Ministry of Education, Science, and Culture, and Grant Po 529/5-1 from the Deutsche Forschungsgemeinschaft (DFG).

References

Arvand A, Bastians H, Welford SM, Thompson AD, Ruderman JV and Denny CT. (1998). *Oncogene*, **17,** 2039–2045.
Arvand A, Welford SM, Teitell MA and Denny CT. (2001). *Cancer Res.*, **61,** 5311–5317.
Bailly RA, Bosselut R, Zucman J, Cormier F, Delattre O, Roussel M, Thomas G and Ghysdael J. (1994). *Mol. Cell. Biol.*, **14,** 3230–3241.
Braun BS, Frieden R, Lessnick SL, May WA and Denny CT. (1995). *Mol. Cell. Biol.*, **15,** 4623–4630.
Brummelkamp TR, Bernards R and Agami R. (2002). *Cancer Cell*, **2,** 243–247.
Chansky HA, Hu M, Hickstein DD and Yang L. (2001). *Cancer Res.*, **61,** 3586–3590.
Dauphinot L, De Oliveira C, Melot T, Sevenet N, Thomas V, Weissman BE and Delattre O. (2001). *Oncogene*, **20,** 3258–3265.
Delattre O, Zucman J, Melot T, Garau XS, Zucker JM, Lenoir GM, Ambros PF, Sheer D, Turc-Carel C, Triche TJ, Aurias A and Thomas G. (1994). *N. Engl. J. Med.*, **331,** 294–299.
Delva L, Gallais I, Guillouf C, Denis N, Orvain C and Moreau-Gachelin F. (2004). *Oncogene*, **23,** 4389–4399.
Deneen B and Denny CT. (2001). *Oncogene*, **20,** 6731–6741.
Deneen B, Hamidi H and Denny CT. (2003a). *Cancer Res.*, **63,** 4268–4274.
Deneen B, Welford SM, Ho T, Hernandez F, Kurland I and Denny CT. (2003b). *Mol. Cell. Biol.*, **23,** 3897–3908.

Dohjima T, Lee NS, Li H, Ohno T and Rossi JJ. (2003). *Mol. Ther.*, **7,** 811–816.
Eliazer S, Spencer J, Ye D, Olson E and Ilaria Jr RL. (2003). *Mol. Cell. Biol.*, **23,** 482–492.
Fuchs B, Inwards CY and Janknecht R. (2003). *FEBS Lett.*, **553,** 104–108.
Fuchs B, Inwards CY and Janknecht R. (2004). *Clin. Cancer Res.*, **10,** 1344–1353.
Fukuma M, Okita H, Hata J and Umezawa A. (2003). *Oncogene*, **22,** 1–9.
Hahm KB, Cho K, Lee C, Im YH, Chang J, Choi SG, Sorensen PH, Thiele CJ and Kim SJ. (1999). *Nat. Genet.*, **23,** 22–227.
Hallier M, Lerga A, Barnache S, Tavitian A and Moreau-Gachelin F. (1998). *J. Biol. Chem.*, **273,** 4838–4842.
Hattinger CM, Potschger U, Tarkkanen M, Squire J, Zielenska M, Kiuru-Kuhlefelt S, Kager L, Thorner P, Knuutila S, Niggli FK, Ambros PF, Gadner H and Betts DR. (2002). *Br. J. Cancer*, **86,** 1763–1769.
Hattinger CM, Rumpler S, Strehl S, Ambros IM, Zoubek A, Potschger U, Gadner H and Ambros PF. (1999). *Genes Chromosomes Cancer*, **24,** 243–254.
Im YH, Kim HT, Lee C, Poulin D, Welford S, Sorensen PH, Denny CT and Kim SJ. (2000). *Cancer Res.*, **60,** 1536–1540.
Kovar H, Jug G, Hattinger C, Spahn L, Aryee DN, Ambros PF, Zoubek A and Gadner H. (2001). *Cancer Res.*, **61,** 5992–5997.
Lessnick SL, Braun BS, Denny CT and May WA. (1995). *Oncogene*, **10,** 423–431.
Lessnick SL, Dacwag CS and Golub TR. (2002). *Cancer Cell*, **1,** 393–401.
Matsui Y, Chansky HA, Barahmand-Pour F, Zielinska-Kwiatkowska A, Tsumaki N, Myoui A, Yoshikawa H, Yang L and Eyre DR. (2003). *J. Biol. Chem.*, **278,** 11369–11375.
May WA, Arvand A, Thompson AD, Braun BS, Wright M and Denny CT. (1997). *Nat. Genet.*, **17,** 495–497.
May WA, Gishizky ML, Lessnick SL, Lunsford LB, Lewis BC, Delattre O, Zucman J, Thomas G and Denny CT. (1993a). *Proc. Natl. Acad. Sci. USA*, **90,** 5752–5756.
May WA, Lessnick SL, Braun BS, Klemsz M, Lewis BC, Lunsford LB, Hromas R and Denny CT. (1993b). *Mol. Cell. Biol.*, **13,** 7393–7398.
Nakatani F, Tanaka K, Sakimura R, Matsumoto Y, Matsunobu T, Li X, Hanada M, Okada T and Iwamoto Y. (2003). *J. Biol. Chem.*, **278,** 15105–15115.
Nishimori H, Sasaki Y, Yoshida K, Irifune H, Zembutsu H, Tanaka T, Aoyama T, Hosaka T, Kawaguchi S, Wada T, Hata J, Toguchida J, Nakamura Y and Tokino T. (2002). *Oncogene*, **21,** 8302–8309.
Ohkura N, Yaguchi H, Tsukada T and Yamaguchi K. (2002). *J. Biol. Chem.*, **277,** 535–543.
Ohno T, Rao VN and Reddy ES. (1993). *Cancer Res.*, **53,** 5859–5863.
Rorie CJ, Thomas VD, Chen P, Pierce HH, O'Bryan JP and Weissman BE. (2004). *Cancer Res.*, **64,** 1266–1277.
Schaefer KL, Brachwitz K, Wai DH, Braun Y, Diallo R, Korsching E, Eisenacher M, Voss R, Van Valen F, Baer C, Selle B, Spahn L, Liao SK, Lee KA, Hogendoorn PC, Reifenberger G, Gabbert HE and Poremba C. (2004). *Cancer Res.*, **64,** 3395–3405.
Spahn L, Petermann R, Siligan C, Schmid JA, Aryee DN and Kovar H. (2002). *Cancer Res.*, **62,** 4583–4587.
Staal A, van Wijnen AJ, Birkenhager JC, Pols HA, Prahl J, DeLuca H, Gaub MP, Lian JB, Stein GS, van Leeuwen JP and Stein JL. (1996). *Mol. Endocrinol.*, **10,** 1444–1456.
Takahashi A, Higashino F, Aoyagi M, Yoshida K, Itoh M, Kyo S, Ohno T, Taira T, Ariga H, Nakajima K, Hatta M, Kobayashi M, Sano H, Kohgo T and Shindoh M. (2003). *Cancer Res.*, **63,** 8338–8344.
Teitell MA, Thompson AD, Sorensen PH, Shimada H, Triche TJ and Denny CT. (1999). *Lab. Invest.*, **79,** 1535–1543.
Thompson AD, Braun BS, Arvand A, Stewart SD, May WA, Chen E, Korenberg J and Denny C. (1996). *Oncogene*, **13,** 2649–2658.
Torchia EC, Jaishankar S and Baker SJ. (2003). *Cancer Res.*, **63,** 3464–3468.
Watanabe G, Nishimori H, Irifune H, Sasaki Y, Ishida S, Zembutsu H, Tanaka T, Kawaguchi S, Wada T, Hata J, Kusakabe M, Yoshida K, Nakamura Y and Tokino T. (2003). *Genes Chromosomes Cancer*, **36,** 224–232.
Watson DK, Robinson L, Hodge DR, Kola I, Papas TS and Seth A. (1997). *Oncogene*, **14,** 213–221.
Weinmann AS and Farnham PJ. (2002). *Methods*, **26,** 37–47.
Wishart MJ and Dixon JE. (1998). *Trends Biochem. Sci.*, **23,** 301–306.
Wishart MJ and Dixon JE. (2002). *Proc. Natl. Acad. Sci. USA*, **99,** 2112–2117.
Zwerner JP, Guimbellot J and May WA. (2003). *Exp. Cell Res.*, **290,** 414–419.